



# Impedance spectroscopy studies of moisture uptake in low-k dielectrics and its relation to reliability



Archana Raja<sup>a</sup>, Robert Laibowitz<sup>b</sup>, Eric G. Liniger<sup>d</sup>, Thomas M. Shaw<sup>d</sup>, Tony F. Heinz<sup>b,c,\*</sup>

<sup>a</sup> Department of Chemistry, Columbia University, New York, NY 10027, United States

<sup>b</sup> Department of Electrical Engineering, Columbia University, New York, NY 10027, United States

<sup>c</sup> Department of Physics, Columbia University, New York, NY 10027, United States

<sup>d</sup> IBM T.J. Watson Research Center, Yorktown Heights, NY 10598, United States

## ARTICLE INFO

### Article history:

Received 20 February 2015

Received in revised form 27 March 2015

Accepted 4 April 2015

Available online 9 April 2015

### Keywords:

Low-k

Impedance spectroscopy

Dielectric relaxation

AC losses

Time dependent dielectric breakdown

Reliability

## ABSTRACT

Assessing the reliability of low dielectric constant materials is an important problem for the scalability of integrated circuits to reduced dimensions. Here we report results of a study of the influence of moisture incursion on dielectric relaxation and reliability in porous low-k (2.55) dielectric constant BEOL capacitors. We apply impedance spectroscopy to measure the dielectric loss tangent as a function of temperature and frequency. From the results, we identify two relaxation modes of water in the porous dielectric, exhibiting thermal activation energies of 0.32 eV and 0.56 eV. Study of the lifetime against time-dependent dielectric breakdown (TDDB) as a function of the dielectric loss tangent measured at AC voltages below 0.5 V yields an inverse power-law relationship. The dielectric loss tangent thus has the potential to serve as a low-voltage test of the susceptibility to early failure and to provide a link between high voltage, accelerated TDDB testing and the underlying physical processes responsible for dielectric breakdown.

© 2015 Elsevier B.V. All rights reserved.

## 1. Introduction

Ultra-low k (ULK) dielectrics are critical for achieving the required performance in advanced integrated circuits. Reduction of the dielectric constant between interconnects in the Back End Of Line (BEOL) alleviates power dissipation and signal delay problems. Porous thin-film materials of dielectric constant as low as 2.4 are currently being employed in the BEOL [1]. Water adsorption by these films can lead to a variety of problems, including increased in-line capacitance and leakage currents, leading in turn to early failure of devices [1,2]. Even under ambient conditions, water can diffuse into the dielectrics on relatively short time scales [2], and Fourier-transform infrared (FTIR) spectroscopy has confirmed the propensity for these materials to absorb moisture [3]. Metallic liner layers that typically separate the dielectric from copper contacts (Fig. 1) have also been reduced in thickness as a consequence of scaling. This leads to the possibility of extrinsic mechanisms for dielectric breakdown, including incorporation of water and the migration of Cu<sup>2+</sup> ions that come in contact with the ULK dielectric at various stages of integration (e.g., in chemical-mechanical

polishing and plasma etching or from aging and defects in sealing) [4]. In a recent report on the switching behavior of memristor metal-oxide-metal structures, water was shown to enhance copper incursion into the oxide [5].

While operating voltages are currently on the order of 1 V, the reliability of the advanced circuits is generally assessed at much higher voltages in accelerated testing. This may cause mechanisms of breakdown that come into play only at lower voltages to be overlooked, as proposed by Muralidhar and co-workers [6]. In this paper, we present measurements of dielectric loss in ULK BEOL capacitors using only low AC voltages (<1 V) and show this to be a sensitive technique that picks up polarization currents caused by even small amounts of water. Thermal activation energies related to the movement of water in nanoporous ULKs can be extracted from the dielectric loss data. An increased loss is also correlated with shorter mean time to failure, signifying potential for low-voltage testing of devices. The activation energies correspond well with the thermal desorption measurements of Proost et al. [7]. This suggests that the dissipative currents are created by local changes in the hydrogen bonds between water molecules and the ULK dielectric. The dynamics of water molecules adsorbed in porous silica has been previously studied using impedance spectroscopy [8–10]. However, the samples under investigation have typically been microporous glass or mesoporous silica particles.

\* Corresponding author at: Department of Electrical Engineering, Columbia University, New York, NY 10027, United States.

E-mail address: [tony.heinz@columbia.edu](mailto:tony.heinz@columbia.edu) (T.F. Heinz).

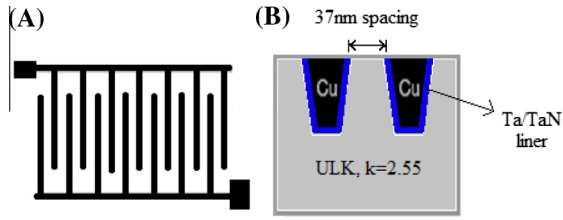


**Fig. 1.** (A) Schematic representation of the top-view of the comb/comb BEOL capacitors investigated in this study. (B) A cross-sectional view of the same structure illustrates the metallized liner layer of Ta/TaN that acts as a diffusion barrier between the copper electrode and porous ULK film.

In this study, we examine porous, ultra-low-k SiCOH [11] capacitors relevant to the microelectronics industry.

## 2. Theoretical background

We have applied impedance spectroscopy to characterize ULK dielectric films and the influence of water on them. In particular, the motion of water molecules can be examined in porous ULK dielectrics using a comb capacitor structure, as shown in Fig. 1. The test structure is modeled as a parallel combination of an ideal capacitor and a lossy resistive component that reflects the dissipative modes in the dielectric. The loss tangent,  $\tan \delta$ , or dissipation factor is the ratio of this resistance to the impedance of the capacitor. In the presence of dissipative channels in the dielectric, the capacitance shows an onset in response with increasing frequency, while the loss tangent exhibits a peak. The peak in the loss is more pronounced than the step in the capacitance and is typically the quantity of choice to measure. In a simple model of the dielectric response, we consider  $N$  discrete relaxation pathways, each with a weight of  $\rho_i$ . From the corresponding frequency dependence of the real and imaginary parts of the dielectric function within a Debye model, we obtain the following expression for the loss tangent [12]:

$$\tan \delta = \frac{(\epsilon_{rs} - \epsilon_{r\infty}) \sum_{i=1}^N \frac{\omega \tau_i \rho_i}{1 + \omega^2 \tau_i^2}}{\epsilon_{r\infty} + (\epsilon_{rs} - \epsilon_{r\infty}) \sum_{i=1}^N \frac{\rho_i}{1 + \omega^2 \tau_i^2}} \quad (1)$$

Here  $\epsilon_{rs}$  and  $\epsilon_{r\infty}$  are the static and high-frequency (relative) dielectric constants of the ULK,  $\omega/2\pi$  is the applied frequency in Hertz, and  $\tau_i$  is the characteristic relaxation time for dissipative mode  $i$  of the molecular motion. For modes that are well separated in energy and occur in different temperature regimes (as relevant below), the peaks in the loss tangent occur for each mode around  $\omega \tau_i = (\epsilon_{rs}/\epsilon_{r\infty})^{0.5}$ .

The temperature dependence of these relaxation times determines the temperature dependence of the loss tangent. We assume a simple, thermally activated model for the variation of the relaxation rate of each mode with the temperature  $T$ :

$$\tau^{-1} = \tau_0^{-1} e^{-E_a/k_B T} \quad (2)$$

Here  $\tau_0$  denotes the relaxation time in the high temperature limit,  $E_a$  is the activation energy for the relevant peak of molecular motion, and  $k_B$  is the Boltzmann constant. Activation energies for different modes can then be determined by the temperature shift in the loss peaks at different applied frequencies. This simple model captures the salient features of the dielectric loss measurement and will be used in interpreting the resulting data in following section.

## 3. Experimental

Interdigitated BEOL comb capacitors, shown schematically in Fig. 1, containing porous ULK of  $k = 2.55$  were provided by IBM. The samples, prepared on 200-mm wafers, were diced into chips and mounted on 24 pin ceramic headers for our measurements. While many metallization layers are used in developing integrated circuits, our test structures consist of a single low-k/metal level, capped with thick metallized silicon oxide that acts as a hermetic seal. The edges of the chip are also sealed with a metallized moisture barrier. The chips typically contain many test structures, including a line of 10 capacitors, with areas varying by more than 3 orders of magnitude. The data in this paper were acquired on the largest two sizes, which have capacitances in the range of 20 pF and 100 pF. The loss tangent as a function of temperature is low ( $\tan \delta \leq 0.001$ ) for capacitors with intact edge seals. Breaks in the edge seal may be introduced during processing, especially as a result of dicing. For this investigation, the edge seals are intentionally scored to expose the ULK comb capacitors to humidity. It was assumed that a 24-h pre-exposure to a particular environment was sufficient to achieve saturation. The measurement of the loss tangent was performed using a HP 4194A impedance analyzer. The samples were placed on a ceramic chip carrier and mounted in a probe station under a nitrogen atmosphere. The temperature was varied from  $-65$  °C to 200 °C using a commercial stage. The applied AC voltages had amplitudes of 0.1–0.5 V in the frequency range of 0.5–500 kHz.

Measurements of time dependent dielectric breakdown (TDDB) lifetime were carried out on 0.1-m long comb/comb test structures using a specially designed test board that can test 8 samples simultaneously in the humidification chamber. TDDB testing was done at the same temperature and relative humidity conditions as the moisture exposure, so that the testing itself would not alter the moisture content of the chips. TDDB testing was carried out at a constant DC voltage of 9.2 V, which represents a nominal field strength of 2.5 MV/cm, based on top line-line spacing of 37 nm. The leakage current was measured as a function of time, with initial leakage on the order of 0.1–1 nA at 9.2 V; breakdown is typically characterized by a jump in leakage current of roughly 6 orders of magnitude. The corresponding failure times are fit using a two-parameter Weibull distribution given by:

$$F(t) = 1 - \exp(-t/\eta)^\beta, \quad (3)$$

where  $\eta$  denotes the scale parameter and  $\beta$  the shape parameter. The Weibull characteristic time,  $T_{63}$ , the time at which 63% of the samples have failed, was determined from (3). In order to display all of the data on a plot representing 25 °C,  $T_{63}$  values measured at 85 °C were corrected to 25 °C by carrying out a separate calibration run in which 8 chips were measured at both temperatures to determine the temperature acceleration factor. To correlate the TDDB lifetime with the amplitude of the dielectric loss, test samples from the same wafer were included in the chamber, to achieve the same exposure to moisture at a given temperature and humidity, but without any applied bias.

## 4. Results and discussion

In Fig. 2 we display the loss tangent measured for our samples at a frequency of 46 kHz over a temperature range from  $-65$  °C to 200 °C. For the temperature and frequency range we observe two dielectric relaxation or dissipation pathways, as indicated by peaks I and II in Fig. 2. By comparison, the as-received samples, with intact edge seals typically show dielectric loss that is  $\leq 0.001$ .

Upon annealing the humidified samples at 200 °C in nitrogen, the low-temperature peak vanishes, while the high-temperature

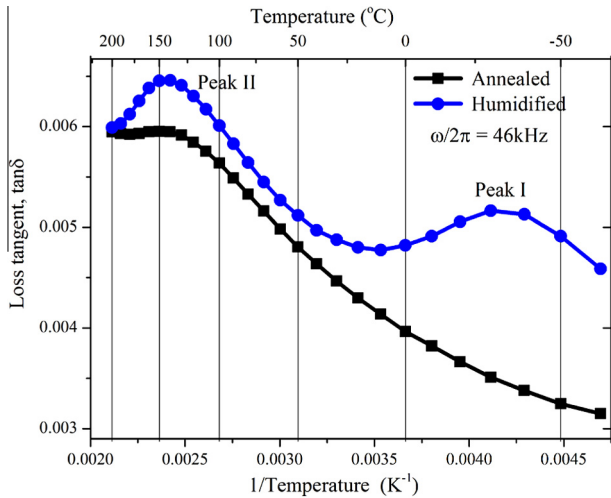


**Fig. 2.** Loss tangent versus temperature at 46 kHz for a sample that was humidified (blue, filled circles) and subsequently annealed (black, filled squares). Peak I occurs around  $-50\text{ }^{\circ}\text{C}$  and peak II at  $150\text{ }^{\circ}\text{C}$ . Annealing the sample at  $200\text{ }^{\circ}\text{C}$  for 2 h in a nitrogen atmosphere removes peak I. (For interpretation of the references to color in this figure legend, the reader is referred to the web version of this article.)

peak, although somewhat reduced in intensity remains. Annealing at  $400\text{ }^{\circ}\text{C}$  for an hour in nitrogen leads to further reduction of the high-temperature peak. Step-wise annealing procedures for ULKs to improve TDDB lifetime, which can be correlated to these relaxation effects, can be found in [13]. We note that the absolute values of the losses are small and the capacitor has a relatively high-Q factor ( $1/\tan\delta$ ), despite diffusion of moisture into the package. The loss peaks also lie on a background that rises with temperature. This can be attributed to a number of factors, including leakage through the device and the tails of higher-energy modes.

The presence of two peaks points to the existence of at least two different types of local environments for water in the ULK, with desorption of the water characterized by peak I occurring during the  $200\text{ }^{\circ}\text{C}$  anneal and peak II at  $400\text{ }^{\circ}\text{C}$ . Upon re-humidifying and annealing the samples at  $200\text{ }^{\circ}\text{C}$ , peak I can be made to appear or disappear, as desired, enabling detailed studies in a non-destructive manner. This suggests that peak I is related to weakly bound water.

For determining the characteristics of peak I, measurements were performed in the temperature range of  $-65$ – $50\text{ }^{\circ}\text{C}$  to avoid loss from water desorption. Before measuring peak II, the sample was annealed for 2 h at  $200\text{ }^{\circ}\text{C}$  in nitrogen to eliminate peak I interference. Normalized dielectric loss data are plotted for the two different modes in Fig. 3(A), demonstrating the shifts in peak position with frequency. The position and amplitude of the peaks, along with the background losses, change with sample history; however, the relative shifts in peak positions for different samples show reproducible Arrhenius behavior, as seen in Fig. 3(B). Thermal activation energies of  $0.32 \pm 0.05\text{ eV}$  and  $0.56 \pm 0.08\text{ eV}$  are obtained for modes I and II, respectively. These are consistent with previous observations in measurements of thermal desorption and mean time to failure measurements [7,14].

While it may not be possible to determine the exact chemical nature of the bonds without further investigation, recent FTIR studies on ULK dielectrics [3], combined with measurements of dielectric relaxation in porous glasses [8–10], suggest that the two observed channels for relaxation in the humidified dielectric can be related to the reorientation of water molecules trapped in the pores. The frequencies and activation energies of the two processes may be associated with relaxation in two different types of silanol environments [7]. In this picture, peak I is linked to “physisorbed” or singly hydrogen bonded water, while peak II with doubly hydrogen bonded or “chemisorbed” water.

A natural question is whether our non-destructive measurements of the loss tangent can be correlated with important dielectric reliability criteria, such as TDDB lifetime.

As illustrated in Fig. 4(A), the AC loss increases with increasing humidity. A dramatic decrease in device lifetime accompanies the increase of the loss, as shown in Fig. 4(B). The Weibull characteristic time ( $T63$ ) has a power-law dependence on the peak dielectric loss of mode I, with the fitted line corresponding to the relation:

$$T63 \sim (\tan\delta)^{-3.08} \tag{4}$$

We thus observe a correlation between device failure and one of the dissipation processes introduced by the presence of water. This result presents a possible path to rapid screening for susceptibility to TDDB failure. Correlating testing with TDDB lifetime at lower voltages may also facilitate the determination of acceleration factors to use conditions. For future studies, since it is known that

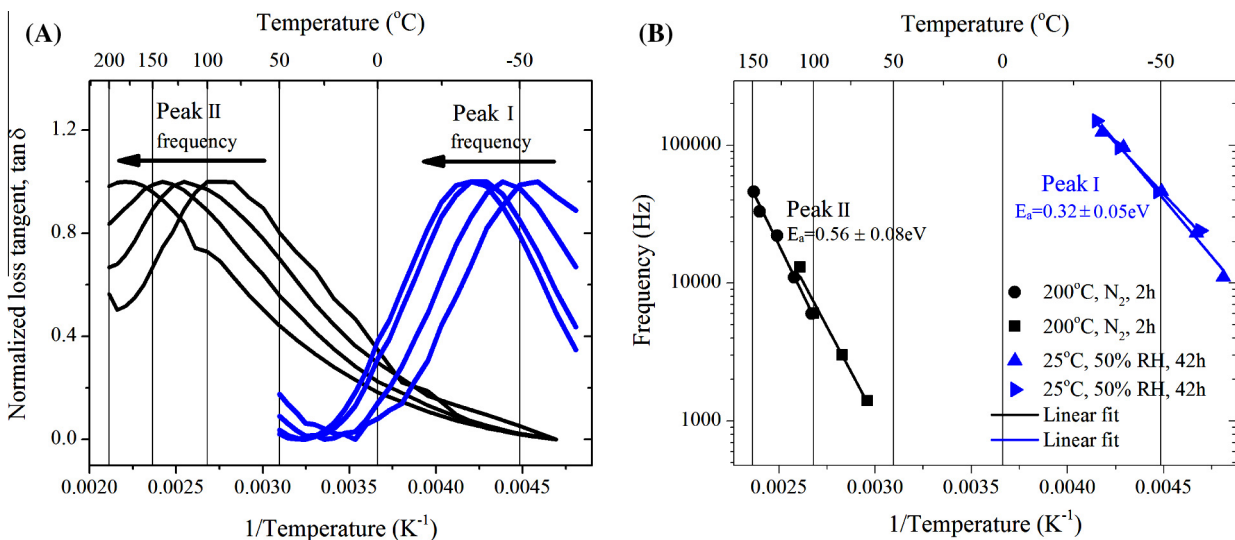


**Fig. 3.** (A) Normalized dielectric loss as a function of inverse temperature, displaying peak shifts for the two dissipation modes at different frequencies. Frequencies for peak I: 22, 46, 96 and 124 kHz, peak II: 5.5, 11, 22 and 46 kHz. (B) Semi-logarithmic plot of frequency versus peak position in inverse temperature, demonstrating Arrhenius behavior over two orders of magnitude of applied frequency for four samples.

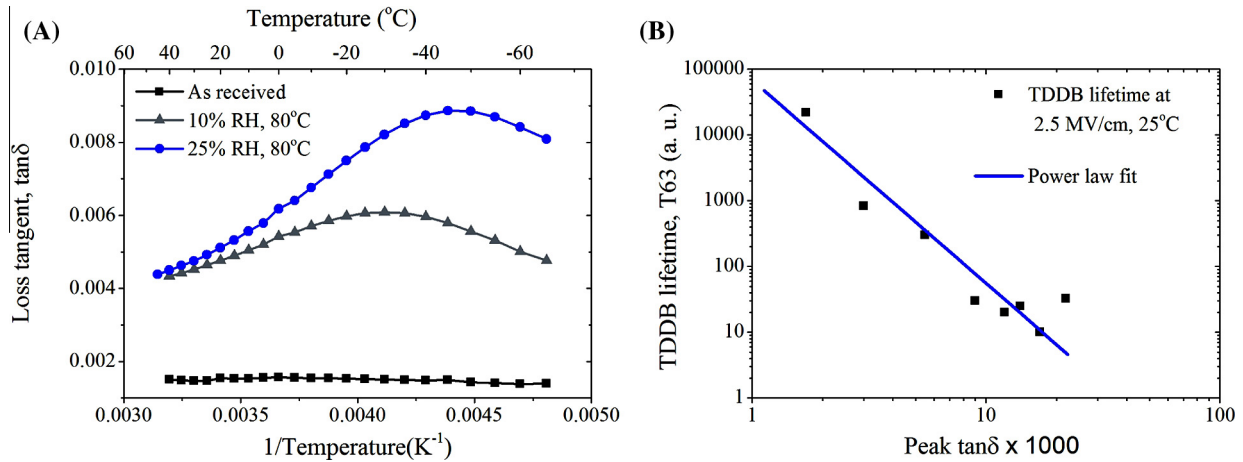


**Fig. 4.** (A) Dielectric loss increases with exposure to increased relative humidity (RH). The capacitor in its as-received state shows low loss. The curves are measured at 87 kHz. (B) TDDDB lifetime is plotted as a function of peak dielectric loss for mode I. Each symbol represents the results of 8 capacitors tested simultaneously at the same relative humidity and temperature. Companion samples obtained from the same wafer were used to measure the dielectric losses plotted along the x-axis. These samples were not biased, but simultaneously exposed to the same humidity and temperature conditions as the TDDDB samples.

annealing at different conditions can lead to different TDDDB lifetimes [4,13], it will be useful to discern the relationship between lifetime and amplitude of the higher temperature dissipation modes.

## 5. Conclusions

The dielectric loss tangent was successfully investigated at low applied voltages for comb capacitors typical of TDDDB test structures. Incorporation of water molecules into the porous dielectric film produced two peaks in the temperature dependence of the loss tangent. Peak I appears at approximately  $-50^{\circ}\text{C}$  and peak II at approximately  $150^{\circ}\text{C}$  at a measurement frequency of 46 kHz. Peak I can be associated with physisorbed water; it is removed by annealing at  $200^{\circ}\text{C}$  in nitrogen and restored by subsequent exposure to moisture. Peak II can be linked to chemisorbed water and requires higher annealing temperatures for removal. We have shown that the amplitude of peak I can be correlated with the TDDDB test lifetime. This indicates the possibility of developing dielectric relaxation as an early indicator of breakdown susceptibility of new processes and materials. The AC testing is performed non-destructively at low voltages, providing a connection between accelerated higher voltage TDDDB testing and mechanisms that are active at lower voltages.

## Acknowledgments

The authors gratefully acknowledge guidance and useful discussions with R. Rosenberg from SUNY CNSE, E. Cartier, R.

Muralidhar, A. Grill and G. Bonilla from IBM and S. King from Intel. This work was supported in part through the Semiconductor Research Corporation (SRC) and the New York CAIST program, task number 1292.072.

## References

- [1] A. Grill, S.M. Gates, T.E. Ryan, S.V. Nguyen, D. Priyadarshini, *Appl. Phys. Rev.* 1 (2014) 011306.
- [2] J.R. Lloyd, T.M. Shaw, E.G. Liniger, *IEEE Int. Integr. Reliab. Workshop Final Rep.* 10598 (2005) 39.
- [3] C. Kubasch, H. Schumacher, H. Ruelke, U. Mayer, J.W. Bartha, *IEEE Trans. Electron Devices* 58 (2011) 2888.
- [4] E.G. Liniger, T.M. Shaw, S.A. Cohen, P.K. Leung, S.M. Gates, G. Bonilla, D.F. Canaperi, S.P. Rao, *Microelectron. Eng.* 92 (2012) 130.
- [5] T. Tsuruoka, K. Terabe, T. Hasegawa, I. Valov, R. Waser, M. Aono, *Adv. Funct. Mater.* 22 (2012) 70.
- [6] R. Muralidhar, T. Shaw, F. Chen, P. Oldiges, D. Edelstein, S. Cohen, R. Achanta, G. Bonilla, M. Bazant, *IEEE Int. Reliab. Phys. Symp.* (2014) 3 (BD 3).
- [7] J. Proost, M. Baklanov, K. Maex, L. Delaey, *J. Vac. Sci. Technol. B* 18 (2000) 303.
- [8] Y. Ryabov, A. Gutina, V. Arkhipov, Y. Feldman, *J. Phys. Chem. B* 105 (2001) 1845.
- [9] A. Spanoudaki, B. Albela, L. Bonneviot, M. Peyrard, *Eur. Phys. J. E* 17 (2005) 21.
- [10] J. Sjöström, J. Swenson, R. Bergman, S. Kittaka, *J. Chem. Phys.* 128 (2008) 154503.
- [11] A. Grill, D.A. Neumayer, *J. Appl. Phys.* 94 (2003) 6697.
- [12] K.C. Kao, *Dielectric Phenomena in Solids*, Academic Press, 2004.
- [13] E.G. Liniger, G. Bonilla, P. Leung, S.A. Cohen, S.M. Gates, T.M. Shaw, *Multiple Step Anneal Method and Semiconductor Formed by Multiple Step Anneal*, U.S. Patent 2013/0049207 A1, 2013.
- [14] Y. Li, I. Ciofi, L. Carbonell, N. Heylen, J. Van Aelst, M.R. Baklanov, G. Groeseneken, K. Maex, Z. Tökei, *J. Appl. Phys.* 104 (2008) 034113.